Analytically Determined Response of a 300-μm Silicon Detector to a Polyenergetic Beam of Neutrons[1]

M. Taherzadeh

Guidance and Control Division

Nuclear radiation from a radioisotope thermoelectric generator used as the prime energy source for electrical power in a space mission could severely affect scientific instruments or detectors on the spacecraft. Therefore, a thorough analysis and evaluation of the types of radiation and their effects on the detectors were necessary.

In this article, the response of a 300-μm silicon detector to an incident polyenergetic neutron beam emitted from a plutonium dioxide fuel power source is determined. The results indicate that the response of the detector is basically due to elastic scattering reactions, and the contribution from other reactions is very small. For neutron energies greater than 4.5 MeV, the (n,p) and (n,α) reactions contribute less than 2% to the total response. The maximum response for this detector is less than 4×10^{-3} counts/neutron within the range of bias energies of 25 to 250 keV. Moreover, this maximum value will decrease if consideration is given to the pulse height defect phenomenon.

Introduction

Nuclear radiation (mainly, neutrons and gamma rays) is emitted when a radioisotope thermoelectric generator is used as the prime energy source for electrical power on a spacecraft. The neutrons and photons are emitted from the plutonium fuel power source with a flux level that depends upon the impurities and the age of the fuel itself. The neutrons interact directly with the spacecraft's scientific instruments or detectors; also, when detectors are shielded against primary photons, additional radiation is generated by inelastic scattering and the radiative capture of the source neutrons within the shield. Since this radiation could severely affect the detectors, it is essential that the types of radiation and their effects on the detectors be thoroughly analyzed and evaluated.

[1]Based on Reference 1.

Response of a Bare Detector

The response of a bare 300-μm silicon detector to neutrons can be studied by an analytical scheme using the probability laws of interactions and energy and angular distributions. In the case of a bare, very thin detector such as discussed here and low-energy neutrons, the pulse height can be estimated easily using kinematical equations. This, of course, does not mean that the exact response can be calculated by such a simplified scheme. Nevertheless, if the response of a silicon detector is estimated for a worst case and shown to be much below the response to the primary gamma rays from the source, the importance of neutrons as far as additional shielding is concerned would be reduced. Since the main emphasis of this analysis is the response to neutrons emanated from a plutonium dioxide fuel power source, the neutron source spectrum is examined first.

The neutron flux and the flux spectrum of a typical plutonium dioxide fuel power source are presented in Figure 1. The fuel is a multihundred-watt (2-kW) power source that emits a total of 4.59×10^4 neutrons/g-s. At 50 cm from the center of the source and at zero angle with respect to the major axis of the fuel, the total flux is 5.43×10^3 neutrons/cm^2-s. From this flux distribution, it is concluded that the average neutron energy is about 2 MeV, and the maximum neutron energy can be as high as 10 MeV or more, but with a very small neutron abundance.

In order to limit the analysis to the number of nuclear reactions involved, a maximum can arbitrarily be set for the neutron energy so that the percent of neutrons to be ignored contributes an insignificant amount to the overall response of the detector. One such arbitrarily selected maximum energy is 6 MeV; the neutrons with energies above this value contribute less than 0.5%.

With a range of energies for the released neutrons having been selected, the response of a silicon detector to a beam of neutrons emitted from a plutonium dioxide fuel power source can now be calculated. The total and the partial neutron cross sections as functions of neutron energies up to 6 MeV (Reference 2) are presented in Figure 2. Elastic scattering (n,n) and inelastic scattering $(n,n'\gamma)$ reactions and (n,α), (n,p), and radiative capture (n,γ) reactions (the neutron disappearing reactions) are considered here. The significant features of these cross sections are:

(1) The (n,p) and (n,α) reactions become important beyond a neutron energy of about 4.5 MeV; however, at these high neutron energies, the neutron abundance diminishes very rapidly. For this reason, reactions that are kinematically possible but have high threshold energies, such as $(n,2n)$ reactions, are not included in this analysis,

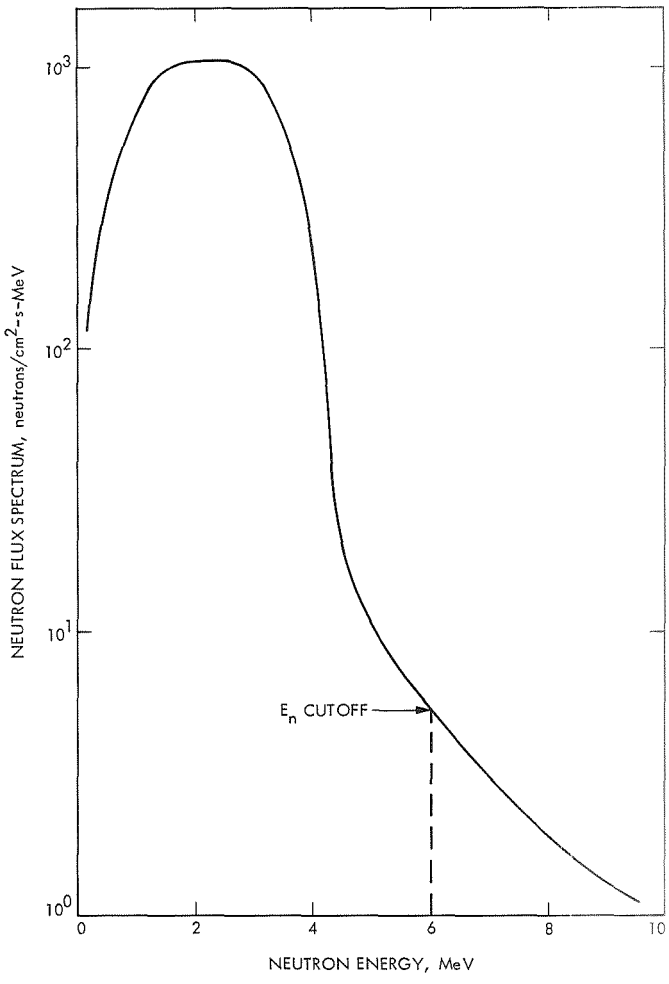

Figure 1. Neutron flux spectrum as a function of neutron energy

and the contributions from such reactions should be considered extremely small.

(2) At low neutron energies (i.e., below 1.5 MeV), only (n,n) and (n,γ) reactions are possible.

(3) In the medium range of neutron energies (i.e., 1.5 to 5 MeV), the difference between the total cross section and the elastic scattering cross section increases with energy, but the difference still remains small. This means that, in this neutron energy range, the (n,n) reaction is the most important.

Thus, the (n,p) and (n,α) reactions can be considered as a source of background, but the (n,n) reaction is by far the largest contributor. The (n,γ) and $(n,n'\gamma)$ reactions have much smaller cross sections, and the

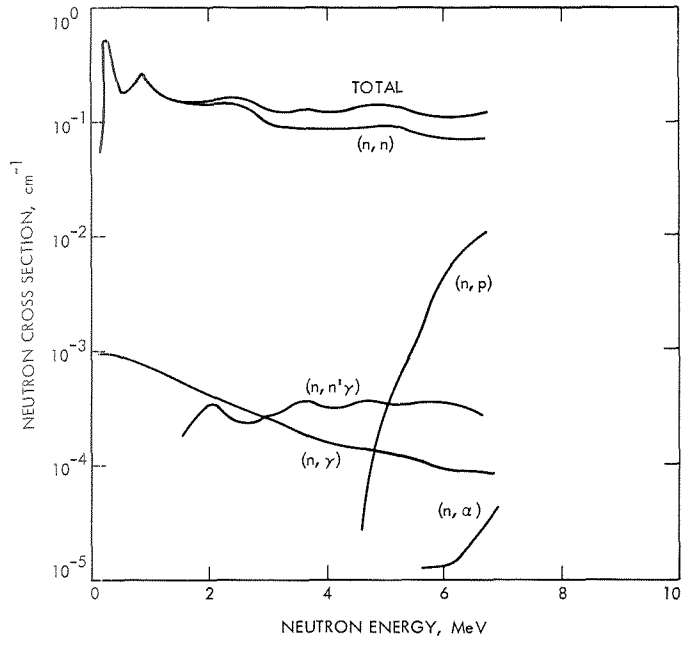

Figure 2. Neutron cross section as a function of neutron energy

emitted photons escape the detector's sensitive area before depositing any energy. In Table 1, the neutron–silicon reactions are listed with their corresponding emitted secondary particles and various characteristics of the reactions. The $(n,2n)$ reaction is included as an example of the reactions that will not be considered due to their high threshold energies and low neutron flux levels.

The response function of a detector medium at a given neutron energy E_n and when angular distribution in the center-of-mass (CM) system is assumed isotropic is given by

$$R(E_n,E_B) = \epsilon_D(E_n) \int_{E_B}^{(E_{Si})_{max}} \frac{dE_{Si}}{\gamma_D E_n} \left[\left(1 - \frac{< \Delta E >}{E_{Si}} \right) \sum_\nu \frac{2\nu + 1}{2} \right.$$

$$\left. \times \alpha_\nu (E_n) P_\nu \left(1 - \frac{2E_{Si}}{\gamma_D E_n} \right) \right] + \epsilon_{\alpha,p}(E_n)\, \delta_{\alpha,p} \qquad (1)$$

where E_B is the bias energy; ϵ terms are efficiency functions; $(E_{Si})_{max}$ is the maximum silicon recoil energy; γ_D is a constant that, for the silicon recoil, is 0.1332; and $< \Delta E > / E_{Si}$ is the fraction of non-ionizing energy dissipated in the medium and, thus, not contributing to the charge collection process of the detector. The P_ν term represents the Legendre polynomials of degree ν, with α_ν as their coefficients; these energy-dependent

Table 1. Characteristics of neutron–silicon reactions[a]

Type of reaction	Specific reaction	Quantity of heat Q, MeV	Threshold neutron energy $(E_n)_{th}$, MeV	Neutron abundance at $(E_n)_{th}$, %	Maximum energy of charged particles, MeV	Range of charged particles, μm	Reaction cross section,[b] $cm^2 \times 10^{-24}$ (=barns)
Neutron disappearing	$Si^{28}(n,\alpha)Mg^{25}$	−2.7	2.66	13	2.68	9	0
Neutron disappearing	$Si^{28}(n,p)Al^{28}$	−3.9	3.66	8.3	1.81	44	0
Elastic scattering	$Si^{28}(n,n)Si^{28}$	0	0	—	0.798	0.045	2.915
Inelastic scattering	$Si^{28}(n,n'\gamma)Si^{28}$	0	0	—	—	—	0.00364
Radiative capture	$Si^{28}(n,\gamma)Si^{29}$	8.47	0	—	—	—	0.0111
Other particle producing	$Si^{29}(n,2n)Si^{28}$	−8.47	8.81	0.14	—	—	0
Other particle producing	$Si^{28}(n,n'p)Al^{27}$	−11.6	12.06	—	—	—	0

[a]Maximum neutron energy $(E_n)_{max} = 6$ MeV.

[b]At 1.5 MeV.

coefficients are obtained from Reference 3, where up to a ninth-order polynomial was used to reproduce the angular distribution of the neutrons. All nine coefficients at any neutron energy are used in this calculation. The $\delta_{\alpha,p}$ term represents the fact that (n,α) and (n,p) reactions can contribute to the total response if $E_{\alpha,p} - < \Delta E >_{\alpha,p} \geq E_B$.

The detector's efficiency function for normal incidence, $\epsilon_D(E_n)$, is generally given by

$$\epsilon_D(E_n) = 1 - \exp\left[-\mu(E_n)t\right] \tag{2}$$

where $\mu(E_n)$ is the attenuation coefficient of the detector and t is the sensitive thickness. The curves for the efficiency functions for (n,n), (n,p), and (n,α) reactions and the curve for the total value for a 300-μm silicon detector are presented in Figure 3. The shape of the curve for the total

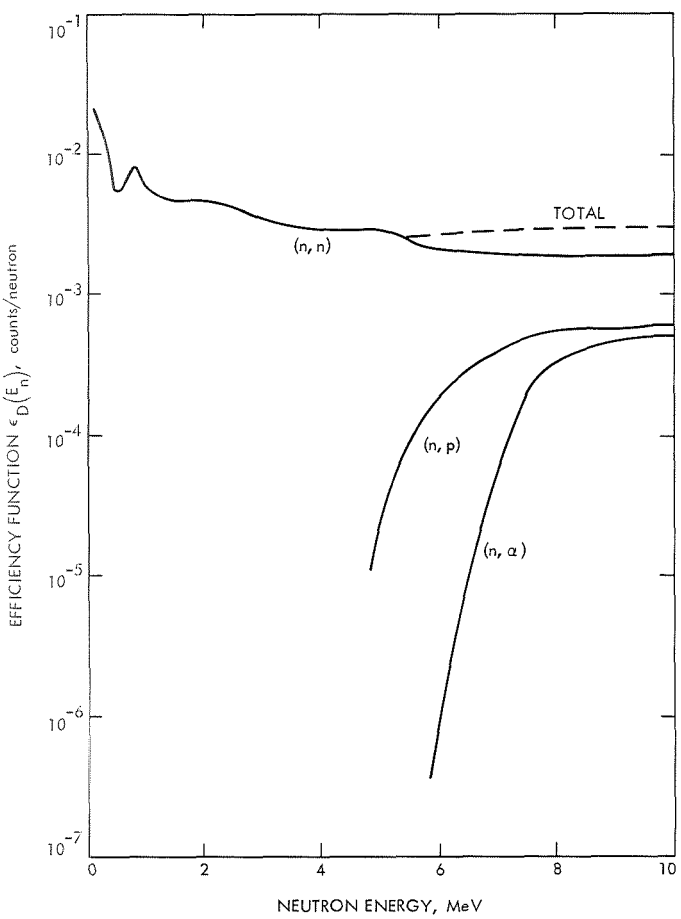

Figure 3. Efficiency function ϵ_D (E_n) as a function of neutron energy

value follows that for the total cross section because the effective thickness of the detector is small and

$$\epsilon_D(E_n) = tN\sigma\,(E_n) \tag{3}$$

where $N\sigma$ is the neutron cross section. Since the energy transferred to the silicon by neutrons is $0.133E_n \sin^2(\theta_{CM}/2)$, where θ_{CM} is the angle in the CM system, $(E_{Si})_{max}$ is obtained when $\nu = 0$, $\theta_{CM} = 180$ deg, and the energy distribution function for the silicon nuclei after collision is $1/(E_{Si})_{max}$. The probability function is given by $1 - [E_B/(E_{Si})_{max}]$, and the response function is

$$R(E_n,E_B) = \epsilon_D(E_n,t)\left(1 - \frac{E_B}{0.133E_{Si}}\right), \qquad \nu = 0 \tag{4}$$

In Figure 4, the response function is plotted for various values of E_n and E_B. The contribution from protons generated in (n,p) reactions and the contribution from alpha particles generated in (n,α) reactions are indeed small. At low E_n, these charged particles do not exist; at high E_n, the contribution from protons is more than one order of magnitude lower and the contribution from alpha particles is about five orders of magnitude lower than the pulse height generated by elastic scattering of neutrons. Therefore, at E_n up to 5 MeV, the major portion (~99%) of

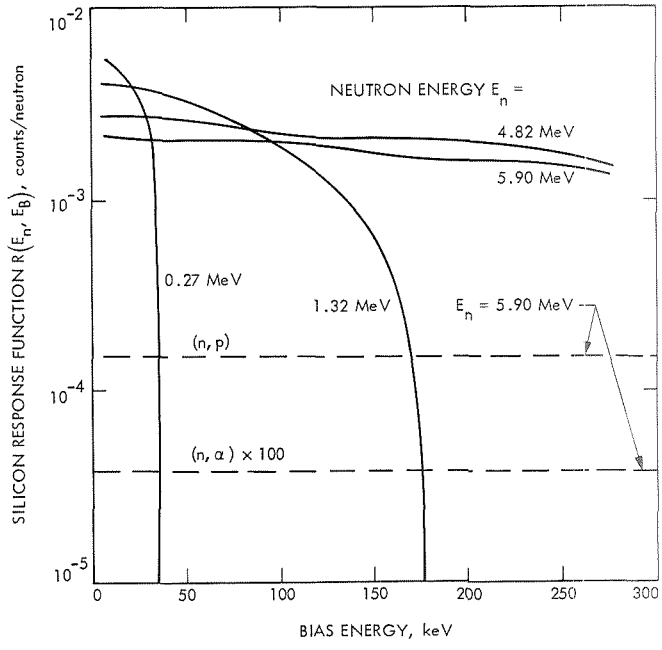

Figure 4. Silicon response function $R\,(E_n, E_B)$ as a function of bias energy

counts comes from the silicon nuclei after being struck by neutrons, and, at 6 MeV, nearly 90% of the response is due to this reaction. The protons and alpha particles generated within the detector are completely absorbed since the edge effects are small. For this reason, they must be included in the pulse height calculation since the time interval for the ionization process is much smaller than the charge collection time interval, and the deposited energy is equal to the maximum energy if it is above E_B.

The neutron flux ϕ from the fuel capsule can also be included in the response function; thus, in the $[0,(E_n)_{max}]$ energy interval, the response of the silicon detector at E_n is

$$\frac{dC(E_n)}{dE_n} = \frac{\phi(E_n)AR(E_n,E_B)}{\phi_0} \tag{5}$$

where A is the detector's cross-sectional area and $dC(E_n/dE_n$ is given in counts/(neutron/cm^2)-MeV. The total silicon counting rate for a polyenergetic neutron beam with energies up to $(E_n)_{max}$ is

$$C(E_n) = \int_{(E_n)_{min}}^{(E_n)_{max}} \phi(E_n)AR(E_n,E_B)dE_n \tag{6}$$

where $(E_n)_{min}$ is the minimum neutron energy allowed for a given E_B (i.e., $7.55E_B$).

Equation 6 is plotted in Figure 5 for the same E_n values used in Figure 4; $C(E_n)$ is given in counts/s for energies from $(E_n)_{min}$ up to $(E_n)_{max}$. The total counting rate at a given E_n depends upon E_B. At $E_B = 100$ keV and $E_n = 5$ MeV, the counting rate is about 20 counts/s when angular distribution is assumed isotropic; no pulse height defects are taken into account, and the total neutron flux for this case is only 151 neutrons/cm^2-s.

Response of a Detector Subject to Pulse Height Defects

The response function calculated in the previous section is yet subject to another restriction, namely, the pulse height defect. This effect is more pronounced in the case of silicon detectors because the pulse height is mainly due to the elastic scattering of neutrons.

Neutrons transfer their energies to the silicon-sensitive medium by atomic scattering and nuclear reactions, rather than through an electronic ionization process. The secondary charged particles produced by the neutron interaction, such as protons, alpha particles, and silicon nuclei,

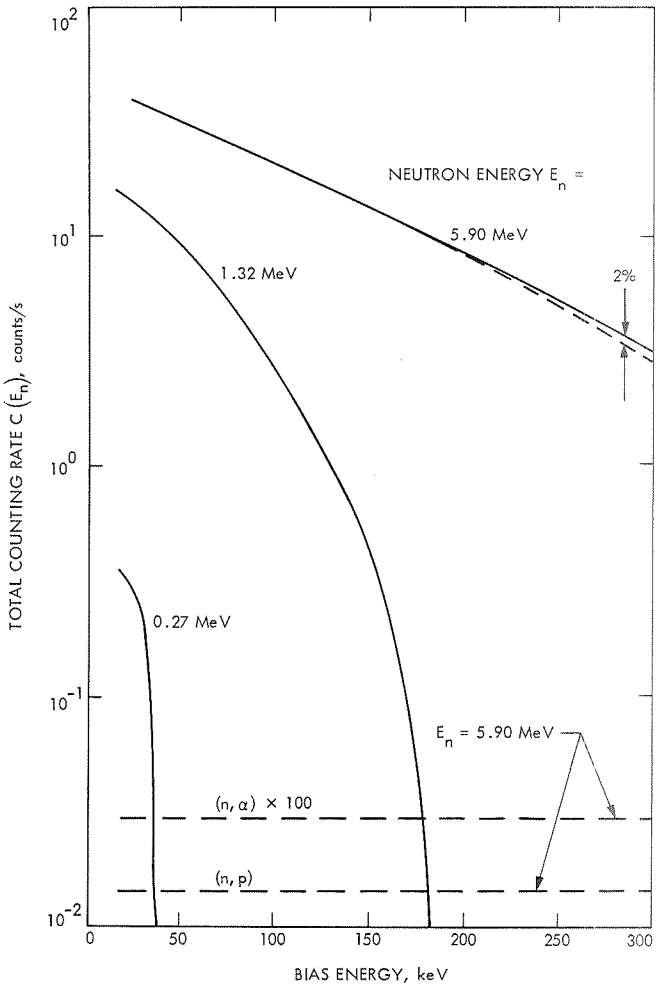

Figure 5. Total counting rate C (E_n) as a function of bias energy

in turn transfer their energies to the medium by ionization and nuclear charge scattering. The photons generated in the (n,γ) and $(n,n'\gamma)$ reactions escape the medium in most cases and thus will not deposit energy. The non-ionizing processes contribute to the pulse height defect. The ionization causes the displacement of electrons, while nuclear charge scattering (Rutherford scattering) causes the displacement of atoms from their equilibrium position and leaves vacancies in the lattice.

The maximum energies and ranges of the protons, alpha particles, and silicon nuclei were presented in Table 1. Since 300 μm was selected as the depletion depth of the detector, nearly all of these charged particles remain inside. The energy transferred to the silicon is $(E^i_{Si})_{max} \sin^2 (\theta_{CM}/2)$, where $(E^i_{Si})_{max}$ is the maximum transmitted energy. If r_i is the ratio of

the mass of the silicon atom to the mass of the ith charged particle (namely, proton, alpha particle, or silicon nucleus), then

$$E_{\mathrm{Si}}^{i} = 4r_i E_i (1 + r_i)^{-2}$$

Since $r_p = 28$, $r_\alpha = 7$, and $r_{\mathrm{Si}} = 1$,

$$(E_{\mathrm{Si}}^{p})_{\max} = 0.1332(E_p)_{\max}$$

$$(E_{\mathrm{Si}}^{\alpha})_{\max} = 0.438(E_\alpha)_{\max}$$

$$(E_{\mathrm{Si}}^{\mathrm{Si}})_{\max} = (E_{\mathrm{Si}})_{\max}$$

If the maximum energies of the charged particles for a 6-MeV neutron beam from Table 1 are used, then

$$(E_{\mathrm{Si}}^{p})_{\max} = 240 \text{ keV}$$

$$(E_{\mathrm{Si}}^{\alpha})_{\max} = 1170 \text{ keV}$$

$$(E_{\mathrm{Si}}^{\mathrm{Si}})_{\max} = 798 \text{ keV}$$

However, in the real case, only fractions of these energies are transmitted to the medium by ionizing processes, and the remainder contribute to the pulse height defect.

Figure 6 presents the fraction of the pulse height defect as a function of the charged particle energy and considers up to two neutron scatters. It may be seen that the pulse height defect is important only at low

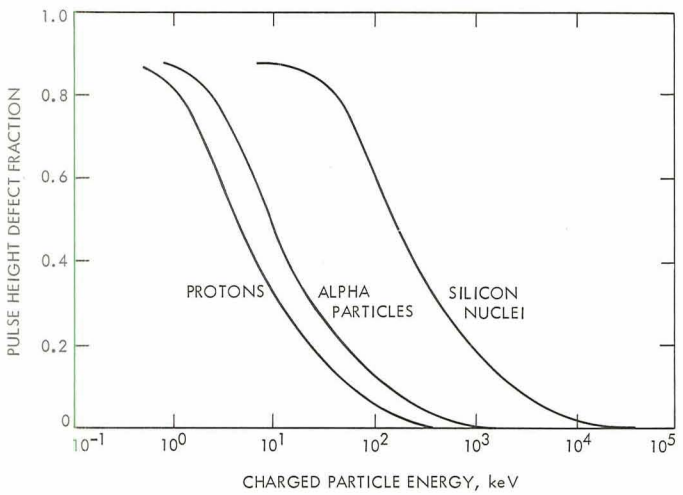

Figure 6. Pulse height defect fraction as a function of charged particle energy

energies, and, within this range, the pulse height defect due to the silicon nuclei is much greater than that due to protons or alpha particles. For example, for a 100-keV charged particle energy ($E_n = 4.5$ MeV for protons, 4.0 MeV for alpha particles, and 0.75 MeV for silicon nuclei), the pulse height defect due to protons is about 6 keV, that due to alpha particles is about 12 keV, and that due to silicon is about 60 keV.

The pulse height defects can now be included in the silicon responses presented in Figure 4. For $E_n = 1.32$ MeV, only silicon nuclei with a maximum energy of 175 keV need to be considered; if E_B is set at higher values, there would be no response. The pulse height defect at this energy (Figure 6) indicates that 58% of the energy is transmitted to the medium by the non-ionizing processes; thus, E_B needs to be set even lower (74 keV) if any response is desired. At high E_n (i.e., 6 MeV), the maximum energies of the charged particles are those given in Table 1, and the pulse height defects are 48 keV for protons, 159 keV for alpha particles, and 528 keV for silicon nuclei. This means that protons and alpha particles will contribute to the total response, but there will be no pulse height due to the (n,n) reaction if $E_B > 270$ keV.

Concluding Remarks

The following remarks summarize the results of this analysis:

(1) For the E_n range of 0.27 to 6 MeV and E_B range of 25 to 250 keV, the maximum response of a 300-μm silicon detector is about 4×10^{-3} counts/neutron.

(2) For an E_n or E_γ of 3 MeV and an E_B of 50 keV, the response of the silicon detector to neutrons is about 11% of the response to the source gamma rays (i.e., $R_n = 0.0029$ and $R_\gamma = 0.025$; Reference 4).

(3) For an E_B range of 50 to 250 keV and for a neutron flux emitted from a multihundred-watt (2-kW) plutonium dioxide fuel power source, the counting rate is estimated to be about 31 to 5 counts/s.

Acknowledgment

The author wishes to express his appreciation to Dr. M. Reier of the JPL Guidance and Control Division for his valuable remarks during this investigation.

References

1. Taherzadeh, M., and Anno, G., "The Response of a 300μ Silicon Detector to Monoenergetic Neutrons Determined by the Use of the

References (contd)

Monte Carlo Technique," paper presented at the National Symposium on Natural and Man-Made Radiation in Space, Las Vegas, Nevada, March 1–5, 1971, sponsored by AEC/NASA (proceedings to be published).

2. Ray, J. W., et al., *Neutron Cross Sections of Nitrogen, Oxygen, Aluminum, Silicon, Iron, Deuterium, and Beryllium,* UNC-5139. United Nuclear Corporation, Elmsford, N.Y., Nov. 1965.

3. Campbell, R. W., et al., *Compilation, Evaluation and Deduction of Neutron Differential Scattering Data, Vol. IV,* NAA-SR-11980. Atomic International, 1967.

4. Reier, M., *The Response of a Shielded 300μ Silicon Detector to Monoenergetic Gamma Rays From 0.279 to 2.75 MeV,* JPL Internal Document EM 342-118. Jet Propulsion Laboratory, Pasadena, Calif., Sept. 14, 1970.